Emergent Cell Subpopulations and Time-Evolving Biophysical Cues in the Developing Porcine Meniscus

Meghan E. Kupratis[1,2], Jiaqi Xiang[3], Kevin G. Burt[1,2], Yuqi Zhang[1], Bryan Kwok[3,4], Sara F. Tufa[5], Douglas R. Keen[5], Nathaniel A. Dyment[1], Lin Han[3], Eiki Koyama[4], Robert L. Mauck[1,2]

[1]University of Pennsylvania, Philadelphia, PA, [2] CMC VA Medical Center, Philadelphia, PA, [3]Drexel University, Philadelphia, PA, [4]The Children's Hospital of Philadelphia, Philadelphia, PA, [5]Shriners Hospital for Children, Portland, OR

meghan.kupratis@pennmedicine.upenn.edu

Disclosures: RL Mauck (5, *4Web Medica*); no other disclosures

INTRODUCTION: Precise cell patterning and extracellular matrix organization are critical to establish and maintain proper function of dense connective tissues, such as the knee meniscus. Although robust, cell-mediated regeneration can occur various fetal connective tissues, this capacity declines rapidly with maturation and is largely absent in the adult meniscus.[1-2] Therefore, defining the molecular pathways and biophysical cues underlying initial formation and expansion of the meniscus during fetal development may reveal new strategies to promote endogenous tissue repair in adults. We demonstrated previously that regionalization of murine meniscus extracellular matrix (ECM) composition and cellular identity are established prenatally,[3-4] and that mechanical forces arising from cellular contraction and muscle loading are required for meniscus patterning and persistence.[5] However, the translatability of the murine model is limited due to the animals' short gestation time, small size, and resultant morphological distinctions relative to humans. To bridge this gap, we recently established a pipeline for timed acquisition of fetal Yorkshire pigs and determined the timing of joint formation and meniscus specification.[6] Here, we expand our porcine model by establishing the single-cell transcriptomic profile of meniscus progenitors as a function of gestational state and quantifying the concurrent emergence and evolution of multiscale ECM structure and micromechanical properties of the developing meniscus.

METHODS: All live animal work was carried out at the National Swine Resource and Research Center (NSRRC, Columbia, MS) under approved protocols. Yorkshire gilts (n=10, ~1yo) were artificially inseminated, and pregnancy was confirmed via ultrasound. Gilts were euthanized during the fifth (embryonic day E34), seventh (E45), ninth (E63-69), twelfth (E84), and sixteenth (P0) weeks of gestation. Animal sex was not delineated for prenatal time points. Hindlimb tissues were collected from the gilts at time of sacrifice. Hind limbs from ≥3 individual fetuses per time point were assayed in all experiments. Freshly isolated menisci were digested for single cell RNA sequencing (scRNA-seq, 10X Genomics).[7-8] Cellularity, proteoglycan distribution, and proteoglycan content were assessed via Safranin-O/Fast Green (SO/FG) and Alcian Blue/Picrosirius Red (AB/PSR) staining. Spatial gene expression was assessed by RNAscope *in situ* hybridization. Phalloidin staining and second harmonic generation (SHG) imaging were used to visualize actin and collagen fibril distribution in the transverse plane. Collagen fibril nanostructure was assessed using transmission electron microscopy (TEM). Atomic force microscopy (AFM) nanoindentation was performed in 1X PBS using polystyrene microspherical tips (Ø25µm, k~0.6N/m), and the effective indentation modulus (E_{ind}) was calculated from the finite thickness-corrected Hertz model. Differences between groups were assessed via two-way ANOVA with multiple comparison-corrected α=0.05.

RESULTS: Single cell transcriptomic profiling of meniscal tissues identified cell populations of mesenchymal, hematopoietic, and endothelial lineages. The majority (>80%) of profiled cells comprised a population enriched for classical fibrochondrocyte markers, including *COL1A1, COL2A1, COMP,* and *TNMD* (**Fig. 1a**). Further analysis of this population revealed distinct subpopulations high in canonical outer zone markers (including *TNMD* and *KERA*) vs. inner zone markers (such as *UCMA* and *TGM2*). The relative proportion of inner zone cells increased during late fetal development, from 10% at E45 to 35% by P0 (**Fig. 1b**). To better understand the spatial variation in these cells' transcriptome, we also sequenced cells from E84 menisci that had been segmented into putative inner and outer zones prior to digestion. In inner zone cells, this analysis uncovered enrichment of a *TNMD*-low population high in chondrogenic markers, including *COL2A1* and *HAPLN1* (**Fig. 1c-d**, cluster 0) and a smaller *TNMD*-low population with high expression of *PRG4* that may correspond to the emerging superficial layer (**Fig. 1c-d**, cluster 4). RNAscope *in situ* hybridization showed *COL2A1, ACAN, and TNMD* expression localized to the outer two-thirds of the meniscus and no staining in the inner zone (**Fig. 1e**). At the nanoscale, collagen fibrils were significantly thicker in the outer meniscus (p<0.0001, **Fig. 2a-b**), and fibril diameter within both regions increased with gestational age (p<0.0001). AFM nanoindentation revealed rapid stiffening of the primitive meniscus during mid- to late-gestation, with E_{ind} increasing 2-fold from E62 to E84 and an additional 3-fold by P0 (p<0.01, **Fig. 2c**). Furthermore, regional micromechanical distinctions were present by E45, such that the outer zone was significantly stiffer than the age-matched inner zone at all time points (p<0.01).

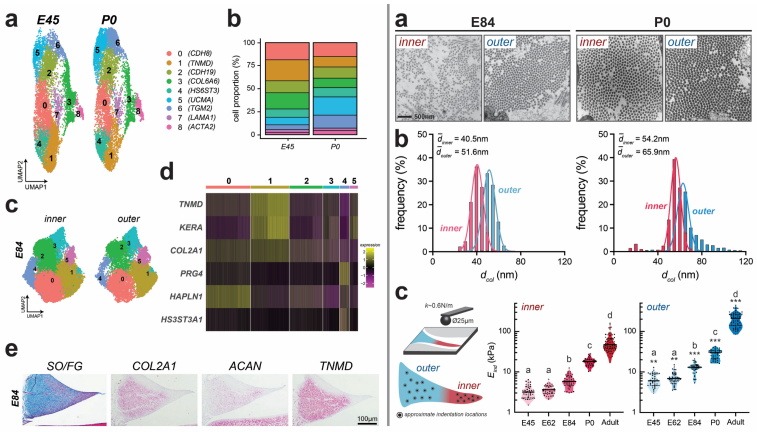

Fig. 1. Single cell transcriptomic analysis of developing meniscus. (a) Subpopulations of MFCs and **(b)** relative proportions, revealing expansion of inner zone cells later in gestation. **(c-d)** Sequencing of segmented inner and outer zone cells identified enrichment of *TNMD*-low cells in the inner zone. **Fig. 2. Nanostructural and micromechanical assessments. (a)** TEM images of E84 and P0 meniscal regions. **(b)** Collagen fibril diameter increased with gestational age and was greater in the outer zone. **(c)** AFM nanoindentation revealed zonal specification at E45 and stiffening within each zone during gestation.

DISCUSSION: This study demonstrates that transcriptional, ultrastructural, and micromechanical regionalization of the primitive meniscus are established early in fetal development. We show that porcine meniscus specialization occurs through rapid microenvironmental refinement during initial tissue formation and gestational growth. Namely, increased transcriptional heterogeneity emerges concurrently with the growth-mediated expansion and refinement of the extracellular matrix during gestation, particularly in the inner zone. Furthermore, high *in situ* expression of *TNMD* in the outer zone shown by RNAscope confirms our scRNA-seq data provides a degree of spatial information. Finally, the observed associations between microstructural and micromechanical properties of the inner and outer zones support a role for mechano-adaptation of meniscus progenitor cells during development. We previously observed greater intrinsic cellular contractility of embryonic porcine cells derived from the outer zone that increases with gestational age.[6] Together with the present findings, this observation suggests that residence within the stiffer, more aligned collagen microenvironment of the outer zone may prime meniscus progenitor cells towards enhanced mechanosensitivity and drive specification of cells distinct from those of the inner zone.

SIGNIFICANCE: This work provides insight to the transcriptional and biophysical mechanisms underlying meniscus formation and regional specification in a large animal model and reveals that regionalization of ECM and resident cells initiates early in embryonic development and is refined during prenatal growth.

REFERENCES: [1] Ionescu+ *Tissue Eng A*, 2011. [2] Qu+ *Sci Rep*, 2018. [3] Tsinman+ *FASEB J*, 2021. [4] Kwok+ *Acta Biomater*, 2023. [5] Tsinman+ *J Orthop Res*, 2023. [6] Kupratis+ *Trans ORS*, 2025. [7] Stuart+ *Cell*, 2019. [8] Knights+ *Ann Rheum Dis*, 2022.

ACKNOWLEDGEMENTS: This work was supported by the NIH (R01AR075418, P30AR069619, S10OD021633). The authors gratefully acknowledge Dr. Kristin Whitworth (NSSRC), Dr. Gordon Ruthel (Penn Vet Imaging Facility), and the CHOP Center for Applied Genomics Sequencing Core.